



Electric Vehicle Charging Station Pricing Control under Balancing Reserve Capacity Commitments

Mladen Čičić, Guillaume Gasnier, Carlos Canudas de Wit

► To cite this version:

Mladen Čičić, Guillaume Gasnier, Carlos Canudas de Wit. Electric Vehicle Charging Station Pricing Control under Balancing Reserve Capacity Commitments. CDC 2023 - 62nd IEEE Conference on Decision and Control, Dec 2023, Singapour, Singapore. pp.1-7. hal-04185104

HAL Id: hal-04185104

<https://hal.science/hal-04185104>

Submitted on 22 Aug 2023

HAL is a multi-disciplinary open access archive for the deposit and dissemination of scientific research documents, whether they are published or not. The documents may come from teaching and research institutions in France or abroad, or from public or private research centers.

L'archive ouverte pluridisciplinaire **HAL**, est destinée au dépôt et à la diffusion de documents scientifiques de niveau recherche, publiés ou non, émanant des établissements d'enseignement et de recherche français ou étrangers, des laboratoires publics ou privés.



Distributed under a Creative Commons Attribution 4.0 International License

Electric Vehicle Charging Station Pricing Control under Balancing Reserve Capacity Commitments

Mladen Čičić, Guillaume Gasnier, Carlos Canudas-de-Wit

Abstract—Electric vehicle charging stations are expected to become key players in the future sustainable power system. We propose a framework for using them to provide balancing services to the grid, by implementing charging price control laws that ensure they are able to deliver their committed balancing capacity. The control laws are based on the Coupled Traffic, Energy, and Charging (CTEC) model, incorporating electric vehicle routing and charging decisions based on the charging price and EV state of charge. Charging stations compete with each other and must ensure a certain number of charging vehicles to maintain their role of frequency containment reserves. The results demonstrate the effectiveness of the proposed pricing control scheme in maximizing charging station profits, without violating their balancing reserve capacity commitments.

I. INTRODUCTION

The increasing prevalence of electric vehicles (EVs), encouraged by governmental policies regarding adoption incentive and charging infrastructure development [1], will have an substantial effect on the power system, as well as the transportation system operation. At the same time, the surge of intermittent renewable energy sources, such as wind and solar, will require an increase in balancing services to maintain grid stability [2]. Therein, battery energy storage systems are essential for providing Frequency Containment Reserves (FCR) due to their quick response time [3]. There is hope that the anticipated large EV fleet could, with appropriate charging coordination, ensure these services without significantly altering their everyday routines.

EV charging stations play an integral role, with different proposed approaches to utilizing them, e.g., considering them as energy storage devices that the operators can use for balancing the grid [4] and reducing renewable energy curtailment [5], or assimilating them into prosumers who interact with the distribution system operator (DSO) in a game-theoretic context [6]. Moreover, the charging price can be used as a control variable to respond to the balancing market [7] or to maximize the charging station profits [8].

These approaches highlight the importance of considering EV charging stations as active participants in the energy system, rather than merely as passive infrastructure. The ability to predict the EV behaviour, in response to e.g. different charging price levels, is essential for charging station coordination. The multinomial logit model [9] provides a good framework for that, through describing the individual EV decisions. This can include predicting which

routes individuals will take [10], as well as when EVs decide to enter and exit a charging station [11], [12].

In this work, we propose a framework for utilizing charging stations to provide balancing services. First, in Section II, we describe the considered electromobility system and outline how charging stations are controlled to achieve our goals, using their charging prices as a control input to ensure that they are capable of providing the contracted reserve capacity. Next, in Section III, we recall the original Coupled Traffic, Energy, and Charging (CTEC) model [13], which describes the EV traffic flows and charging dynamics. One contribution of this work is in extending the model to a general road network structure, as well as in incorporating the EV routing and charging decisions considering their State of Charge (SoC) and charging station price. Then, in Section IV, we analyse the model and design charging station pricing control laws, which is another contribution of this work. We propose a simple linear control law, and an optimization-based control law, designed to maximize charging station profits while ensuring the charging stations do not violate their reserve capacity commitments. Finally, in Section V, the proposed control laws are put to the test in simulations, demonstrating good performance, and their effectiveness is compared. We conclude the paper in Section VI by summarizing its results and discussing possible directions for future work.

II. ELECTROMOBILITY BALANCING SERVICES

The outline of the studied electromobility system used to provide balancing services is shown in Fig. 1. We extend the CTEC model [13] to capture the effect of EV routing and charging decisions, based on their SoC and the charging prices at all charging stations in the road network. The control is executed in a decentralized manner, with each

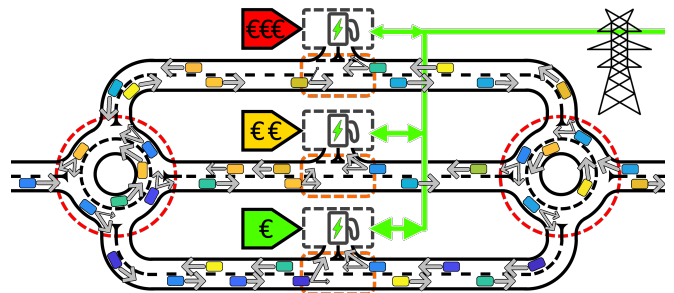


Fig. 1: Sketch of the studied electromobility system. EVs make decisions when they approach interchanges (outlined in dashed red) and junctions connected to charging stations (dashed orange) based on their SoC (warmer colours indicate higher SoC), the traffic conditions, and the charging prices.

charging station choosing its price without knowing how the other charging stations' prices will change. The ability of charging stations to change their power consumption and provide FCR depends directly on the number of EVs present. Charging stations are therefore competing to attracting EV traffic, and will need to reduce their prices in order to be able to provide enough balancing capacity.

The system studied in this work consists of three routes with road links heading in both directions, connecting two interchanges. At the two interchanges, a portion of EVs leave the system, and a constant flow of new EVs enters the system. The EVs at the interchanges then decide which one of the three links leading towards the other interchange to take, based on the traffic conditions and charging prices of the different routes, and then continue driving. At the middle of each route, there is a public charging station which EVs on the links of that route can enter if they decide to go charge, based on their SoC and the charging price. After charging, the EVs continue their trips in the same direction, by returning to the appropriate road link.

For each charging station $\zeta \in \mathcal{Z}$, where \mathcal{Z} is the set of all charging stations, the charging price $u_\zeta(t)$ is changed with the time step of $T = 1$ h, $u_\zeta(t) = u_\zeta(kT)$, $kT \leq t < (k+1)T$. This control time step is equal to the time steps of the electricity price $\pi(t)$ and FCR commitments for downward regulation $\mathcal{P}_\zeta^\downarrow(t)$ and upward regulation $\mathcal{P}_\zeta^\uparrow(t)$. Each charging station $\zeta \in \mathcal{Z}$ is required to change its power consumption $P_\zeta(t)$ from its nominal power $\tilde{P}_\zeta(t)$ to its prescribed regulation profile $P_\zeta^*(t)$,

$$P_\zeta^*(t) = \tilde{P}_\zeta(t) + \begin{cases} R_\zeta^\uparrow(t) \mathcal{P}_\zeta^\downarrow(t), & R_\zeta^\uparrow(t) \geq 0, \\ R_\zeta^\downarrow(t) \mathcal{P}_\zeta^\uparrow(t), & R_\zeta^\downarrow(t) < 0, \end{cases} \quad (1)$$

where $-1 \leq R_\zeta^\uparrow(t) \leq 1$ shapes the downward (\downarrow) and upward (\uparrow) balancing actions. In case of downward regulation, we have $\mathcal{P}_\zeta^\downarrow(t) \geq 0$, i.e., the charging station is required to be able to increase its power consumption (equivalent to decreasing power generation) by $\mathcal{P}_\zeta^\downarrow(t)$ when requested, and in case of upward regulation, the charging station must be able to decrease its power consumption (increase power generation), $\mathcal{P}_\zeta^\uparrow(t) \leq 0$, potentially even returning energy to the grid through vehicle-to-grid (V2G). If the charging station is unable to follow its assigned power consumption reference, it violates its FCR commitments which would incur large penalties, so the control laws must be designed in a way that makes these events rare.

III. MODEL

In this section we introduce the extended CTEC model used in this work. We first present the traffic density and SoC model on links and junctions of the network, then introduce the charging station model, and finally complete the model by discussing the decisions of the EVs.

A. Combined traffic and energy model

Consider a road network described by a directed graph $(\mathcal{J}, \mathcal{L})$, where \mathcal{J} is the set of road junctions (graph nodes) and \mathcal{L} the set of road links (graph edges). The evolution of the EV traffic state in space x and time t on road link $l \in \mathcal{L}$,

consisting of its traffic density $\rho_l(x, t)$ and SoC $\varepsilon_l(x, t) \in [0, 1]$, is given by

$$\begin{aligned} \frac{\partial \rho_l(x, t)}{\partial t} + \frac{\partial (v_l(x, t) \rho_l(x, t))}{\partial x} &= 0, \\ \frac{\partial \varepsilon_l(x, t)}{\partial t} + v_l(x, t) \frac{\partial \varepsilon_l(x, t)}{\partial x} &= \mathcal{D}(v_l(x, t)), \end{aligned}$$

for $0 < x < X_l$, where X_l is the length of link l , together with the boundary conditions at $x = 0$ and $x = X_l$. Here, $v_l(x, t)$ denotes the traffic speed which directly depends on the traffic density, $v_l(x, t) = \mathcal{V}(\rho_l(x, t))$, and $\mathcal{D}(v)$ is the battery discharge function, describing the rate of change of the SoC of an EV, given its speed v . Equivalently, we may define the dependence of the traffic flow $q_l(x, t)$ on the traffic density, $q_l(x, t) = Q(\rho_l(x, t))$, according to the *fundamental diagram* $Q(\rho) = \mathcal{V}(\rho)\rho$, and get the traffic speed as $q_l(x, t) = v_l(x, t)\rho_l(x, t)$.

For each junction $j \in \mathcal{J}$, we denote the set of links entering it by \mathcal{L}_j^- , and the set of links exiting it by \mathcal{L}_j^+ . Since we assume that neither vehicles nor energy can accumulate at any of the junctions, the inflow and outflow of both the traffic and the energy are equal,

$$\begin{aligned} \sum_{l \in \mathcal{L}_j^-} q_l(X_l, t) - q_j^{\text{off}}(t) &= \sum_{l \in \mathcal{L}_j^+} q_l(0, t) - q_l^{\text{on}}(t), \quad j \in \mathcal{J}, \\ \sum_{l \in \mathcal{L}_j^-} q_l(X_l, t) \varepsilon_l(X_l, t) - q_l^{\text{off}}(t) \varepsilon_l^{\text{off}}(t) &= \dots \\ &= \sum_{l \in \mathcal{L}_j^+} q_l(0, t) \varepsilon_l(0, t) - q_l^{\text{on}}(t) \varepsilon_l^{\text{on}}(t), \quad j \in \mathcal{J}. \end{aligned}$$

The entrance of EVs into the road network via junction j , entering links $l \in \mathcal{L}_j^+$, is described exogenously, through its on-ramp flow $q_l^{\text{on}}(t)$ and SoC $\varepsilon_l^{\text{on}}(t)$. Conversely, the exit of EVs from the road network via junction j , is defined by its off-ramp flow $q_l^{\text{off}}(t)$ and SoC $\varepsilon_l^{\text{off}}(t)$, $l \in \mathcal{L}_j^-$, which are a function of the traffic and energy state at the downstream boundary of their respective links l , $\rho(X_l, t)$ and $\varepsilon(X_l, t)$.

In this work, we consider two types of junctions: interchanges and junctions connected to charging stations. At interchanges, we have multiple links entering and exiting the junction, and on- and off-ramp flows connecting the system with the *outside world*. The on-ramp flows of interchanges are defined exogeneously by $q_l^{\text{on}}(t)$ and $\varepsilon_l^{\text{on}}(t)$, for all $l \in \mathcal{L}_j^+$. A portion of the flow reaching the interchange junction on each link $l^- \in \mathcal{L}_j^-$ exits the system via the off-ramp,

$$q_l^{\text{off}}(t) = \beta_j q_l^-(X_l^-, t), \quad \varepsilon_l^{\text{off}}(t) = \varepsilon_l^-(X_l^-, t),$$

defined by the constant splitting ratio β_j , and the remainder of the incoming traffic flow is distributed to links $l^+ \in \mathcal{L}_j^+$,

$$\begin{aligned} q_{l^+}(0, t) &= (1 - \beta_j) \sum_{i \in \mathcal{L}_j^-} q_i(X_i, t) \lambda_i^{l^+}(t), \\ q_{l^+}(0, t) \varepsilon_{l^+}(0, t) &= (1 - \beta_j) \sum_{i \in \mathcal{L}_j^-} q_i(X_i, t) \varepsilon_i(X_i, t) \lambda_i^{l^+}(t). \end{aligned}$$

Splitting ratios $\lambda_i^{l^+}(t)$ are the result of the EV routing decisions which will be discussed at the end of this section.

At junctions connected to charging stations, we have a single link entering and a single link leaving the junction, and the on- and off-ramp flows connect the road network to

a charging station, serving as a link between the road and the charging station parts of the CTEC model. These flows, as well as the EV decisions related to charging stations, will be discussed in the remainder of this section.

B. Charging station model

The state of each charging station $\zeta \in \mathcal{Z}$ is defined by the concentration of EVs present at different levels of SoC $\eta_\zeta(\varepsilon, t)$. The evolution of $\eta_\zeta(\varepsilon, t)$ is given by

$$\frac{\partial \eta_\zeta(\varepsilon, t)}{\partial t} + \frac{\partial (c_\zeta(\varepsilon, t) \eta_\zeta(\varepsilon, t))}{\partial \varepsilon} = \mu_\zeta^{\text{in}}(\varepsilon, t) - \mu_\zeta^{\text{out}}(\varepsilon, t),$$

where $c_\zeta(\varepsilon, t)$ denotes the rate at which the EVs are charging, $\mu_\zeta^{\text{in}}(\varepsilon, t)$ denotes the flow of EVs entering the charging station, and $\mu_\zeta^{\text{out}}(\varepsilon, t)$ the flow of EVs exiting it. These flows are defined as a function of the on- and off-ramp flows of the junction ζ connected to the charging station ζ (note the slight abuse of notation), according to

$$\mu_\zeta^{\text{in}}(\varepsilon, t) = \sum_{l \in \mathcal{L}_\zeta^-} \delta(\varepsilon - \varepsilon_l^{\text{off}}(t)) q_l^{\text{off}}(t),$$

where $\delta(x)$ is the Dirac delta function, and

$$q_\zeta^{\text{on}}(t) = \int_0^1 \mu_\zeta^{\text{out}}(\varepsilon, t) d\varepsilon, \quad q_\zeta^{\text{on}}(t) \varepsilon_\zeta^{\text{on}} = \int_0^1 \varepsilon \mu_\zeta^{\text{out}}(\varepsilon, t) d\varepsilon.$$

For each charging station $\zeta \in \mathcal{Z}$, we define the minimum, nominal, and maximum charging rate \underline{C}_ζ , \tilde{C}_ζ , and \overline{C}_ζ , respectively, $\underline{C}_\zeta \leq 0 \leq \tilde{C}_\zeta \leq \overline{C}_\zeta$. In order to make the charging station more appealing to the EVs considering charging, we guarantee that they will be charged at least at the nominal rate \tilde{C}_ζ until they reach some limit SoC $\tilde{\varepsilon}$. To this end, we split the vehicles present at charging station ζ into those with *low* SoC (less than the limit value $\varepsilon < \tilde{\varepsilon}$), and those with *high* SoC ($\varepsilon \geq \tilde{\varepsilon}$). The number of EVs with low and high SoC, $\eta_\zeta^{\text{lo}}(t)$ and $\eta_\zeta^{\text{hi}}(t)$, respectively, is thus

$$\eta_\zeta^{\text{lo}}(t) = \int_0^{\tilde{\varepsilon}} \eta_\zeta(\varepsilon, t) d\varepsilon, \quad \eta_\zeta^{\text{hi}}(t) = \int_{\tilde{\varepsilon}}^1 \eta_\zeta(\varepsilon, t) d\varepsilon,$$

and we write these two condensed states jointly as $N_\zeta(t) = [\eta_\zeta^{\text{lo}}(t) \quad \eta_\zeta^{\text{hi}}(t)]^\top$. The charging rates of different vehicles groups (“lo” and “hi”) are thus defined as

$$c_\zeta(\varepsilon, t) = \begin{cases} \max\{0, c_\zeta^{\text{lo}}(t)\}, & \varepsilon = 0, \\ c_\zeta^{\text{lo}}(t), & 0 < \varepsilon < \tilde{\varepsilon}, \\ c_\zeta^{\text{hi}}(t), & \tilde{\varepsilon} \leq \varepsilon < 1, \\ \min\{0, c_\zeta^{\text{hi}}(t)\}, & \varepsilon = 1. \end{cases}$$

These two charging rates take values in $\tilde{C}_\zeta \leq c_\zeta^{\text{lo}}(t) \leq \overline{C}_\zeta$ and $\underline{C}_\zeta \leq c_\zeta^{\text{hi}}(t) \leq \overline{C}_\zeta$, respecting the guarantee, depending on the reference value of power that the charging station ζ should attempt to achieve, as described below.

We define the power consumption of charging station ζ as

$$P_\zeta(t) = \int_0^1 c_\zeta(\varepsilon, t) \eta_\zeta(\varepsilon, t) E d\varepsilon,$$

where E denotes the EV battery average capacity. Note that since $\underline{C}_\zeta \leq 0$, we may have $P_\zeta(t) < 0$, representing V2G flow of energy from the EVs at the charging station to the grid. Charging rates $c_\zeta^{\text{lo}}(t)$ and $c_\zeta^{\text{hi}}(t)$ are given by a heuristic similar to the one in [5], prioritizing charging the vehicles

with low SoC over charging those with high SoC,

$$c_\zeta^{\text{lo}}(t) = \begin{cases} \tilde{C}_\zeta, & P_\zeta^*(t) < \tilde{P}_\zeta(t), \\ \max\left\{\tilde{C}_\zeta, \min\left\{\frac{P_\zeta^*(t) - \eta_\zeta^{\text{hi}}(t) \tilde{C}_\zeta E}{\eta_\zeta^{\text{lo}}(t) E}, \overline{C}_\zeta\right\}\right\}, & P_\zeta^*(t) \geq \tilde{P}_\zeta(t), \end{cases}$$

$$c_\zeta^{\text{hi}}(t) = \begin{cases} \max\left\{\underline{C}_\zeta, \min\left\{\frac{P_\zeta^*(t) - \eta_\zeta^{\text{lo}}(t) \underline{C}_\zeta E}{\eta_\zeta^{\text{hi}}(t) E}, \tilde{C}_\zeta\right\}\right\}, & P_\zeta^*(t) < \tilde{P}_\zeta(t), \\ \min\left\{\overline{C}_\zeta, \max\left\{\frac{P_\zeta^*(t) - \eta_\zeta^{\text{lo}}(t) \overline{C}_\zeta E}{\eta_\zeta^{\text{hi}}(t) E}, \tilde{C}_\zeta\right\}\right\}, & P_\zeta^*(t) \geq \tilde{P}_\zeta(t), \end{cases}$$

where $P_\zeta^*(t)$ is the reference power (1) provided by the grid operator to the charging station ζ . Using these charging rates, the minimum, nominal, and maximum charging station power are defined as

$$\underline{P}_\zeta(t) = E[\underline{C}_\zeta \quad \underline{C}_\zeta] N_\zeta(t), \quad (2)$$

$$\tilde{P}_\zeta(t) = E \tilde{C}_\zeta \mathbb{1}^\top N_\zeta(t), \quad (3)$$

$$\overline{P}_\zeta(t) = E \overline{C}_\zeta \mathbb{1}^\top N_\zeta(t), \quad (4)$$

respectively, where $\mathbb{1}$ is a column vector of all 1-s of appropriate dimension, assuming $\eta_\zeta(1, t) = 0$. It can be verified that for $P_\zeta^*(t) = \tilde{P}_\zeta(t)$ we have $c_\zeta^{\text{lo}}(t) = c_\zeta^{\text{hi}}(t) = \tilde{C}_\zeta$.

However, if $R_\zeta^\dagger(t) \neq 0$, it is possible that the charging station ζ violates its FCR commitments when $P_\zeta^*(t) < \underline{P}_\zeta(t)$ or $P_\zeta^*(t) > \overline{P}_\zeta(t)$, due to the limitations on $c_\zeta^{\text{lo}}(t)$ and $c_\zeta^{\text{hi}}(t)$,

C. EV decisions model

The model is completed by describing the aggregate influence of the decisions that the EVs make in their daily operation, by defining the relevant splitting ratios. Namely, the EVs need to decide when to enter the charging station, and which route to take, and base their decision on their current SoC, traffic conditions, and price of charging of different charging stations. We adopt three modelling assumptions:

- Lower SoC makes the EVs more likely to enter the charging station.
- Higher charging price makes the EVs less likely to enter the charging station.
- If the EVs have a low SoC and can choose between multiple charging stations, they are more likely to go to the charging station with a lower price.

Since human behaviour is notoriously difficult to model, in this work we propose and use simple behavioural heuristic, which enable us to analyse the system while still respecting the three stated assumptions. The dependence of the relevant splitting ratios on the charging price is illustrated in Fig. 2.

As EVs reach the charging station ζ on link $l \in \mathcal{L}_\zeta^-$, they have to make a decision on whether to enter it and charge, or continue driving and defer charging. We assume this decision depends only on their current SoC $\varepsilon_l(X_l, t)$ and the current charging price $u_\zeta(t)$. The outcome is modelled through the splitting ratio towards the charging station

$$\beta_\zeta(\varepsilon_l(X_l, t), u_\zeta(t)) = 1 - \left(1 + e^{-\frac{\varepsilon_l(X_l, t) - (U_0 + U_1 u_\zeta(t))}{\gamma_\zeta}}\right)^{-1},$$

where γ_ζ is a scaling constant, $U_0 + U_1 u_\zeta(t)$ is the threshold SoC indicating the level below which vehicles are more likely

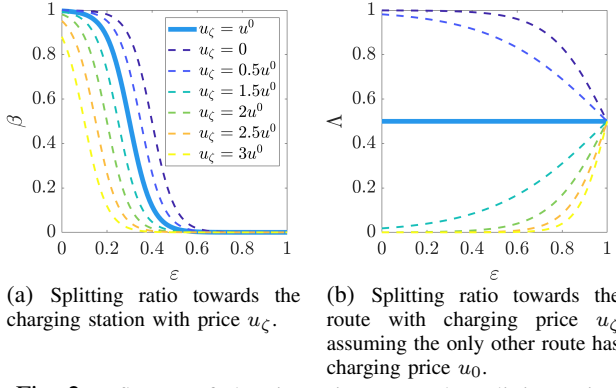


Fig. 2: Influence of charging price u_c on the splitting ratios.

than not to enter the charging station, and U_0 and U_1 are constant parameters. Since the number of vehicles entering the charging station is expected to decrease as the charging price increases, we have $U_1 < 0$.

EVs also need to decide when to leave the charging station. For simplicity, we assume this happens as soon as they are fully charged,

$$\mu_{\zeta}^{\text{out}}(\varepsilon, t) = \delta(\varepsilon - (1-))c_{\zeta}(\varepsilon, t)\eta_{\zeta}(\varepsilon, t),$$

where $1-$ indicates a point arbitrarily close to 1 from the left, yielding $q_{\zeta}^{\text{on}}(t) = c_{\zeta}^{\text{hi}}(t)\eta_{\zeta}(1-, t)$ and $\varepsilon_{\zeta}^{\text{on}}(t) = 1$.

Finally, EVs need to decide what route to take when they reach an interchange. We associate a score

$$\Lambda_{l^-}^{l^+}(t) = w_{\theta}\theta_{l^+}(t) + w_u(1 - \varepsilon_{l^-}(X_{l^-}, t))u_{\zeta_{l^+}}(t),$$

with each link $l^+ \in \mathcal{L}_j^+$ exiting the interchange, indicating its overall desirability to EVs approaching from link $l^- \in \mathcal{L}_j^-$, which is used to determine their splitting ratio towards it. Here, $\theta_{l^+}(t)$ denotes the travel time of link l^+ at time t , $u_{\zeta_{l^+}}(t)$ is the charging price of charging station ζ_{l^+} connected to link l^+ , and $w_{\theta} < 0$ and $w_u < 0$ are the constant weights of the two terms. Therefore, following [9], the splitting ratio of EVs arriving via link l^- towards link l^+ is given by

$$\lambda_{l^-}^{l^+}(t) = \frac{e^{\Lambda_{l^-}^{l^+}(t)}}{\sum_{i \in \mathcal{L}_j^+} e^{\Lambda_{l^-}^{i}(t)}}. \quad (5)$$

IV. CONTROL DESIGN

In this section we propose control laws for charging station ζ using the charging price $u_{\zeta}(t)$ to maximize its profit while respecting its FCR commitments $\mathcal{P}_{\zeta}^{\uparrow}(t)$ and $\mathcal{P}_{\zeta}^{\downarrow}(t)$. Note that the time step used here, $T = 1$ h, is significantly slower than the dynamics of the system. We first linearize the model, then give a simple control law based on satisfying the FCR commitments, and finally introduce a prediction-based optimal pricing control law. Both of the proposed control laws are required to ensure the charging station respects its FCR capacity commitments

$$\bar{P}_{\zeta}(t) - \bar{P}_{\zeta}(t) \leq \mathcal{P}_{\zeta}^{\uparrow}(t), \quad (6)$$

$$\bar{P}_{\zeta}(t) - \bar{P}_{\zeta}(t) \geq \mathcal{P}_{\zeta}^{\downarrow}(t). \quad (7)$$

A. Model linearization

Due to the long control interval T , high complexity of the model, as well as the inherent uncertainty related to the decisions of the EVs and other charging stations, it is very

hard to find the required predictions of the evolution of $N_{\zeta}(t)$ for $kT < t \leq (k+1)T$. Instead, a simplified linearized model of the charging station dynamics is used for control.

Considering the charging station model presented in Section III-B, the evolution of $N_{\zeta}(t)$ are approximated as

$$\dot{N}_{\zeta}(t) \approx AN_{\zeta}(t) + B\hat{\mu}_{\zeta}^{\text{in}}(t)$$

where matrices A and B are given by

$$A = \begin{bmatrix} -\frac{\bar{C}}{\bar{\varepsilon} - \hat{\varepsilon}} & 0 \\ \frac{\bar{C}}{\bar{\varepsilon} - \hat{\varepsilon}} & -\frac{\bar{C}}{1 - \hat{\varepsilon}} \end{bmatrix}, \quad B = \begin{bmatrix} 1 \\ 0 \end{bmatrix},$$

and $\hat{\varepsilon}$ is the average SoC of the EVs entering the charging station. The total inflow of EVs to the charging station $\hat{\mu}_{\zeta}^{\text{in}}(t)$ can be written as

$$\hat{\mu}_{\zeta}^{\text{in}}(t) = \Delta_{\zeta}(t) + M_{\zeta}(t)u_{\zeta}(t), \quad (8)$$

where $u_{\zeta}(t)$ is the charging price, and $\Delta_{\zeta}(t)$ the aggregated disturbance originating from model linearization errors and uncertainty about the traffic conditions. We represent the influence that an increase in price $u_{\zeta}(t)$ has on the inflow of EVs to the charging station by $M_{\zeta}(t)$, $M_{\zeta}(t) \leq 0$, depending on the situation in the rest of the system. Note that $\Delta_{\zeta}(t) > 0$ has a non-zero mean, since it represents the average inflow to charging station ζ in case of $u_{\zeta}(t) = 0$.

Due to the nature of the linearized system, and piecewise-constant $u_{\zeta}(t) = u_{\zeta}(kT)$, $kT < t \leq (k+1)T$, it is enough to evaluate $N_{\zeta}(t)$ at the end of the control interval. We predict $N_{\zeta}((k+1)T)$ approximately as

$$N_{\zeta}((k+1)T) \approx e^{AT}N_{\zeta}(kT) + \hat{A}_T B(\underline{\Delta}_{\zeta}(k) + \underline{M}_{\zeta}(k)u_{\zeta}(kT)), \quad (9)$$

where $\underline{\Delta}_{\zeta}(k) = \frac{1}{T} \int_{kT}^{(k+1)T} \Delta_{\zeta}(t) dt$, $\underline{M}_{\zeta}(k) = \frac{1}{T} \int_{kT}^{(k+1)T} M_{\zeta}(t) dt$, and \hat{A}_T is given by

$$\hat{A}_T = \int_0^T e^{At} dt = A^{-1}(e^{AT} - I).$$

Finally, we need to determine the parameters of the inflow of EVs to each charging station $\zeta \in \mathcal{Z}$, $\underline{\Delta}_{\zeta}(k)$ and $\underline{M}_{\zeta}(k)$. The total EV flow entering charging station ζ , (8), is written

$$\hat{\mu}_{\zeta}^{\text{in}}(kT + \tau) = \sum_{l \in \mathcal{L}_{\zeta}^-} q_l(X_l, kT + \tau) \beta_{\zeta}(\varepsilon_l(X_l, kT + \tau), u_{\zeta}(kT)),$$

for $0 \leq \tau < T$ where, \mathcal{L}_{ζ}^- is the set of all links from which EVs enter charging station ζ . This expression can be simplified in the steady state case, where we assume the EVs traverse these links at a constant speed, $v_l(x, t) = \frac{X_l}{\theta_l(t)}$, that the total traffic flow circulating in the network, i.e., approaching all charging stations from both interchanges, is approximately constant, $\sum_{\zeta \in \mathcal{Z}} \sum_{l \in \mathcal{L}_{\zeta}^-} q_l(0, t) \approx \hat{q}$, and that the SoC of EVs arriving at the charging station is also approximately constant, $\varepsilon_l(X_l, t) \approx \hat{\varepsilon}$. In this case, we may approximate the total number of EVs that enters charging station ζ during $kT \leq t < (k+1)T$ as

$$\hat{\mu}_{\zeta}^{\text{in}}(k) \approx \beta_{\zeta}(\hat{\varepsilon}, u_{\zeta}(kT)) \left((T - \hat{\theta}_{\zeta}(k)) \hat{\lambda}_{\zeta}(k) + \hat{\theta}_{\zeta}(k) \hat{\lambda}_{\zeta}(k-1) \right) \hat{q}, \quad (10)$$

where $\hat{\theta}_{\zeta}(k)$ is the average travel time from the interchanges to the charging station ζ at time $t = kT$, and $\hat{\lambda}_{\zeta}(k)$ is

$$\hat{\lambda}_{\zeta}(k) = \frac{e^{w_{\theta} \hat{\theta}_{\zeta}(k) + w_u(1 - \hat{\varepsilon})u_{\zeta}(kT)}}{\sum_{i \in \mathcal{Z}} e^{w_{\theta} \hat{\theta}_i(k) + w_u(1 - \hat{\varepsilon})u_i(kT)}},$$

which is a special case of the routing decision model (5). Note that $\hat{\mu}_\zeta^{\text{in}}(k)$ therefore depends not only on $u_\zeta(kT)$, but also on the charging price of other charging stations. Finally, we linearize (10) around $u_\zeta(kT) \approx \hat{u}_\zeta(k)$, $\zeta \in \mathcal{Z}$, yielding

$$\begin{aligned} \underline{M}(k) &= \left(\frac{\partial \hat{\mu}_\zeta^{\text{in}}(k)}{\partial u_\zeta(kT)} \right) \bigg|_{u_\zeta(kT) = \hat{u}_\zeta(k), \zeta \in \mathcal{Z}}, \\ \underline{\Delta}(k) &= \left(\hat{\mu}_\zeta^{\text{in}}(k) - \underline{M}(k) u_\zeta(kT) \right) \bigg|_{u_\zeta(kT) = \hat{u}_\zeta(k), \zeta \in \mathcal{Z}}. \end{aligned}$$

The choice of the linearization prices $\hat{u}_\zeta(k)$ has a significant impact on the quality of inflow prediction. Since charging station ζ does not know what the next charging price of other charging stations will be, we linearize $\hat{\mu}_\zeta^{\text{in}}(k)$ around

$$\hat{u}_\zeta(k) = \alpha_u u_\zeta((k-1)T),$$

where $0 < \alpha_u < 1$, in order to improve robustness. By selecting a lower α_u we adopt the pessimistic assumption that the other charging stations will reduce their price for the coming hour, thus making it harder for charging station ζ to attract more EVs.

B. Commitment-satisfaction control

Having linearized the model, we are now able to propose a simple control law which uses feedforward to satisfy constraints (6) and (7), and feedback to suppress the effect of variations in the aggregate disturbance $\Delta(t)$. Substituting (2), (3), (4), and (9) into (6) and (7), and assuming $\underline{\Delta}(t) = 0$, these constraints can be approximated to

$$\left(\underline{C}_\zeta - \tilde{C}_\zeta \right) E \begin{bmatrix} 0 & 1 \end{bmatrix} \left(e^{AT} N_\zeta(kT) + \hat{A}_T B \hat{\mu}_\zeta^{\text{in}}(kT) \right) \leq \underline{P}_\zeta^\dagger(k),$$

$$\left(\bar{C}_\zeta - \tilde{C}_\zeta \right) E \mathbf{1}^\top \left(e^{AT} N_\zeta(kT) + \hat{A}_T B \hat{\mu}_\zeta^{\text{in}}(kT) \right) \geq \bar{P}_\zeta^\dagger(k).$$

Here, $\underline{P}_\zeta^\dagger(k)$ and $\bar{P}_\zeta^\dagger(k)$ are the more stringent constraints between those at kT and $(k+1)T$,

$$\underline{P}_\zeta^\dagger(k) = \alpha_P \min \left\{ \underline{P}_\zeta^\dagger(kT), \underline{P}_\zeta^\dagger((k+1)T) \right\},$$

$$\bar{P}_\zeta^\dagger(k) = \alpha_P \max \left\{ \bar{P}_\zeta^\dagger(kT), \bar{P}_\zeta^\dagger((k+1)T) \right\},$$

multiplied by some constant $\alpha_P > 1$ to improve robustness to disturbance by tightening the constraints.

Both of these constraints are satisfied if $u_\zeta(kT)$ is chosen such that $\hat{\mu}_\zeta^{\text{in}}(kT) \geq \hat{\mu}_\zeta^{\text{in}\dagger}(k)$, where

$$\hat{\mu}_\zeta^{\text{in}\dagger}(k) = \max \left\{ \hat{\mu}_\zeta^{\text{in}\uparrow}(k), \hat{\mu}_\zeta^{\text{in}\downarrow}(k) \right\}, \quad (11)$$

and $\hat{\mu}_\zeta^{\text{in}\uparrow}(k)$ and $\hat{\mu}_\zeta^{\text{in}\downarrow}(k)$ are the minimum inflows to charging station ζ that will cause constraints (6) and (7) to be satisfied, respectively

$$\hat{\mu}_\zeta^{\text{in}\uparrow}(k) = \frac{\underline{P}_\zeta^\dagger(k)}{(\underline{C}_\zeta - \tilde{C}_\zeta)E} - \begin{bmatrix} 0 & 1 \end{bmatrix} e^{AT} N_\zeta(kT) \bigg/ \begin{bmatrix} 0 & 1 \end{bmatrix} \hat{A}_T B,$$

$$\hat{\mu}_\zeta^{\text{in}\downarrow}(k) = \frac{\bar{P}_\zeta^\dagger(k)}{(\bar{C}_\zeta - \tilde{C}_\zeta)E} - \mathbf{1}^\top e^{AT} N_\zeta(kT) \bigg/ \mathbf{1}^\top \hat{A}_T B.$$

Finally, the commitment-satisfaction control law is given by

$$u_\zeta(kT) = \frac{1}{\underline{M}_\zeta(k)} \left(\hat{\mu}_\zeta^{\text{in}\dagger}(k) - \underline{\Delta}_\zeta(k) \right).$$

C. Optimal pricing control

At every time $t = kT$, the optimal pricing control law aims to calculate the updated charging price for the next interval, $u_\zeta(kT)$, so that the profit of charging station is maximized and so that it respects its FCR commitments. This is achieved by solving the maximization problem

$$\begin{aligned} & \max_{u_\zeta(kT)} J_\zeta(k) \\ & \text{s.t. model dynamics} \\ & \text{FCR capacity commitments} \\ & \mathbf{1}^\top N_\zeta(t) \leq \bar{N}_\zeta \\ & kT < t \leq (k+1)T \end{aligned} \quad (12)$$

with the utility function $J_\zeta(k)$ reflecting the hourly profit of charging station ζ ,

$$J_\zeta(k) = (u_\zeta(kT) - \pi(k)) \int_{kT}^{(k+1)T} \tilde{P}_\zeta(t) dt, \quad (13)$$

where $\pi(k)$ is the price of electricity for $kT \leq t < (k+1)T$.

Following the discussion from the previous section, constraints (6) and (7), modelling the FCR capacity commitments, can be rewritten as constraints on the charging price $u_\zeta(kT)$

$$u_\zeta(kT) \leq \frac{1}{\underline{M}_\zeta(k)} \left(\hat{\mu}_\zeta^{\text{in}\dagger}(k) - \underline{\Delta}_\zeta(k) \right),$$

where $\hat{\mu}_\zeta^{\text{in}\dagger}(k)$ is the more restrictive minimum inflow (11).

Similarly, the charging station capacity constraint (12) can be rewritten as

$$\mathbf{1}^\top \left(e^{AT} N_\zeta(kT) + \hat{A}_T B (\underline{\Delta}_\zeta(k) + \underline{M}_\zeta(k) u_\zeta(kT)) \right) \leq \bar{N}_\zeta.$$

Since the nominal power $\tilde{P}_\zeta(t)$ depends directly on $N_\zeta(t)$ according to (3), considering (9) we have

$$\int_{kT}^{(k+1)T} N_\zeta(t) dt \approx \hat{A}_T N_\zeta(kT) + A^{-1} (\hat{A}_T - TI) B (\underline{\Delta}_\zeta(k) + \underline{M}_\zeta(k) u_\zeta(kT)),$$

and therefore cost function (13) can be approximated by

$$J'_\zeta(k) = \alpha_2(k) u_\zeta^2(kT) + \alpha_1(k) u_\zeta(kT) \approx J_\zeta(k),$$

where the current coefficients $\alpha_1(k)$ and $\alpha_2(k)$ are

$$\alpha_1(k) = \mathbf{1}^\top \left(\hat{A}_T N_\zeta(kT) + A^{-1} (\hat{A}_T - TI) B (\underline{\Delta}_\zeta(k) - \underline{M}_\zeta(k) \pi(k)) \right),$$

$$\alpha_2(k) = \mathbf{1}^\top A^{-1} (\hat{A}_T - TI) B \underline{M}_\zeta(k).$$

The optimization problem that is solved in order to acquire the control simplifies to

$$\max_{u_\zeta(kT)} \alpha_2(k) u_\zeta^2(kT) + \alpha_1(k) u_\zeta(kT)$$

$$\text{s.t. } u_\zeta(kT) \leq \frac{1}{\underline{M}_\zeta(k)} \left(\hat{\mu}_\zeta^{\text{in}\dagger}(k) - \underline{\Delta}_\zeta(k) \right)$$

$$u_\zeta(kT) \leq \frac{1}{\underline{M}_\zeta(k)} \left(\hat{\mu}_\zeta^{\text{in}\downarrow}(k) - \underline{\Delta}_\zeta(k) \right)$$

$$u_\zeta(kT) \geq \frac{1}{\underline{M}_\zeta(k)} \left(\frac{\bar{N}_\zeta - \mathbf{1}^\top e^{AT} N_\zeta(kT)}{\mathbf{1}^\top \hat{A}_T B} - \underline{\Delta}_\zeta(k) \right)$$

It can be shown that $\alpha_2(k) < 0$, resulting in a convex optimization problem, which are easy to solve.

V. SIMULATION RESULTS

Finally, we test the proposed charging station pricing control laws for providing balancing services, in simulations

of the set-up outlined in Section II and Figure 1. The main simulation parameters are given in Table I.

The considered road network consists of 8 junctions, of which 2 interchanges and 6 charging station off-ramps, with 3 routes connecting the 2 interchanges (j_1 and j_2) in both directions, formed of 12 links (4 links per route, $j_1 \rightarrow \zeta_i$, $\zeta_i \rightarrow j_2$, $j_2 \rightarrow \zeta_i$, and $\zeta_i \rightarrow j_1$). Formally, there are 6 charging stations, but the pairs of virtual charging stations associated to each route are considered jointly as one charging station.

The simulation model is initialized with uniformly distributed initial traffic density $\rho_l(x, 0) \in [6, 13.5]$ veh/km, uniformly distributed initial SoC $\varepsilon_l(x, 0) \in [0.4, 0.6]$, and $\eta_\zeta(\varepsilon, 0) = 0$ veh. The dynamics of EV traffic are described by an exponential traffic speed function

$$\mathcal{V}(\rho) = v_{\text{ff}} e^{-\frac{1}{2} \left(\frac{\rho}{\rho_{\text{cr}}} \right)^2}$$

with free flow speed of $v_{\text{ff}} = 100$ km/h and critical density of $\rho_{\text{cr}} = 15$ veh/km, and a second-order polynomial battery discharge function

$$\mathcal{D}(v) = D_0 + D_1 v + D_2 v^2$$

with parameters $D_0 = 0.0175$ 1/h, $D_1 = 3 \cdot 10^{-3}$ 1/km, and $D_2 = 2.15 \cdot 10^{-5}$ h/km². In order to initialize the system, the charging price of all charging stations is kept constant for the first two hours, and their balancing capacity is kept at zero for that time.

Charging stations with three different pricing strategies are competing against each other:

- 1) Constant price, not providing balancing services
- 2) Commitment-satisfaction controlled price, providing balancing services
- 3) Optimally controlled price, providing balancing services.

The latter two control schemes are described in Section IV-B and Section IV-C, respectively. The hourly committed balancing capacities of both charging stations are randomly generated day-ahead, with $\mathcal{P}_\zeta^\downarrow(kT)$ and $\mathcal{P}_\zeta^\uparrow(kT)$ uniformly distributed in $[0, \bar{P}]$ MW and $[-\bar{P}, 0]$ MW, respectively. The charging stations' FCR are activated at random times $R_\zeta^\uparrow(t)$, generated as a Poisson arrival process with an average gap of 1 h. At each FCR activation event, it is equally likely that the request is for upward (with $R_\zeta^\uparrow(t) < 0$) and downward ($R_\zeta^\uparrow(t) > 0$) regulation. The hourly price at which the charging stations buy electricity $\pi(kT)$ is known ahead of time, and is uniformly distributed in $[4, 10]$.

We executed five simulation batches, with 100 runs of 24 hours each, using different maximum balancing capacity commitments $\bar{P} \in \{0, 0.1, 0.2, 0.3, 0.4\}$ MW. The results are shown in Figure 3, displaying the first, second, and third

Symbol	Value	Unit	Symbol	Value	Unit
X_l	25	km	U_0	0.4	1
T	1	h	U_1	-0.0125	1/EUR
E	60	kWh	w_θ	-36	1/h
\bar{C}_ζ	-0.83	1/h	w_u	-1	1/EUR
\hat{C}_ζ	0.83	1/h	$\hat{\varepsilon}$	0.45	1
\bar{C}_ζ	1.67	1/h	\hat{q}	4600	veh/h
\bar{N}_ζ	50	veh	α_u	0.8	1
$\bar{\varepsilon}$	0.7	1	α_P	1.2	1

TABLE I: Simulation parameters and their values.

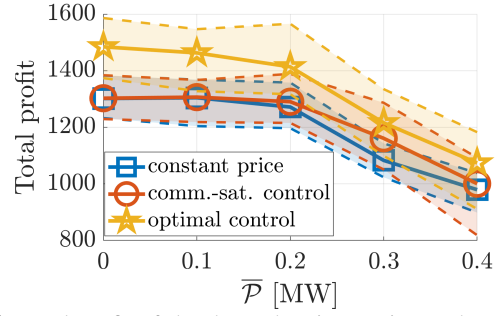
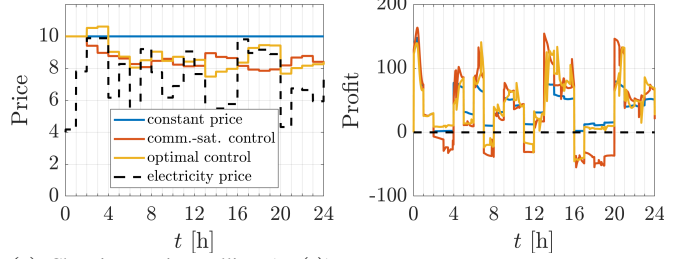


Fig. 3: Total profit of the three charging stations. The solid lines show the median profits over all simulation runs, and the range between the first and third quartile is shaded and outlined dashed.



(a) Charging station selling ($u_c(t)$) and buying ($\pi(t)$) electricity prices.

(b) Charging station profits.

Fig. 4: Charging station prices and profits.

quartile of the total profit achieved by different charging stations. Since the commitment-satisfaction price control law is designed solely to ensure that the balancing capacity commitments are respected, applying it in case of a very low \bar{P} leads to bad results. Therefore, the charging price of the second charging station is set to the same nominal value as that of the first one for $\bar{P} = 0$ MW and $\bar{P} = 0.1$ MW.

It can be seen from Fig. 3 that the profit of all charging stations decreases as the committed balancing capacity increases, requiring more competitive pricing to ensure that the commitments are satisfied. This is the case even for the charging station with constant price, since the other two charging stations will need to reduce their prices in order to attract enough EVs. Note that in this case the revenue that the charging stations would get for providing FCR is not included in the profit, hence the total achieved profit will be higher. The charging station with optimal pricing consistently achieves the best profit. However, in case of $\bar{P} = 0.4$ MW, this charging station slightly violates the balancing commitments, with average and maximum cumulative violation of 0.0711 MWh and 0.717 MWh, respectively, over the full simulation run. In practice, these violations could be offset using stationary storage, or by better selecting of balancing capacity commitments to match the expected EV traffic conditions.

In order to better demonstrate the operation of the model and the control laws, we display the details of one simulation run with $\bar{P} = 0.4$ MW. In Fig. 4 we show the charging and electricity prices, as well as charging station profits over time, and in Fig. 5 the evolution of charging station power over the course of the simulation run. The spikes in charging station power are due to the arrival of requests for downward (in case of the increase of power) and upward (in case of the

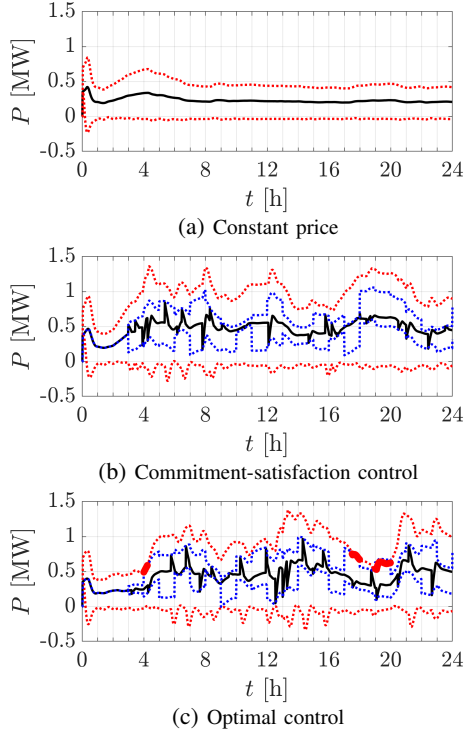


Fig. 5: Current charging station power $P_\zeta(t)$ (black), maximum ($\bar{P}_\zeta(t)$) and minimum ($\underline{P}_\zeta(t)$) achievable power (dotted red), and committed range of reference power for downward ($\bar{P}_\zeta(t) + \mathcal{P}_\zeta^\downarrow(t)$) and upward ($\underline{P}_\zeta(t) + \mathcal{P}_\zeta^\uparrow(t)$) regulation (dotted blue). Thick red line indicates times when the FCR commitment is violated.

decrease) regulation. As shown in Fig. 5c, the optimal pricing control does violate the balancing capacity commitments, but in practice, this violation is very small, with total energy of 0.2629 MWh. As a result of lower conservatism, allowing higher charging prices, the optimal pricing control achieves around 20% higher profit than the commitment-satisfaction control in this case.

VI. CONCLUSIONS

In this work we proposed a framework for EV charging station pricing control for maximizing their profit, while ensuring they can provide FCR. We extend the CTEC model to the case of the road network, as well as to explicitly capture the influence that the charging price has on EV decisions, and design the pricing control laws based on the linearization of the model. Charging stations with different control laws are made to compete against each other in the simulations, and are in general shown to be able to respect most of their balancing capacity commitments, while achieving better profit than the benchmark charging station with constant charging price. It was shown that the FCR commitments by the charging stations requires them to reduce their charging price, potentially leading to cheaper service for the consumers, while also helping the power grid.

This work aims to provide the theoretical framework for the discussed problem, and as such includes the necessary

simplifying assumptions about the power and transportation grid etc. In the future, all facets of the overall system will need to be considered in more detail. The dynamics of the EV traffic and the influence that the altered routing behaviour will have on it is among the topics that need to be addressed. On the other side, a more realistic representation of the power grid and its complexities will need to be considered explicitly. Finally, practical aspects of implementing FCR via EV charging stations need to be tackled, and the potential contribution of such schemes to building a more sustainable future need to be assessed.

REFERENCES

- [1] G. Conway, A. Joshi, F. Leach, A. García, and P. K. Senecal, "A review of current and future powertrain technologies and trends in 2020," *Transportation Engineering*, vol. 5, p. 100 080, 2021.
- [2] M. Esteban, J. Portugal-Pereira, B. C. McLellan, *et al.*, "100% renewable energy system in japan: Smoothing and ancillary services," *Applied energy*, vol. 224, pp. 698–707, 2018.
- [3] A. Oudalov, D. Chartouni, and C. Ohler, "Optimizing a battery energy storage system for primary frequency control," *IEEE Transactions on power systems*, vol. 22, no. 3, pp. 1259–1266, 2007.
- [4] P. H. Divshali and C. Evens, "Optimum day-ahead bidding profiles of electrical vehicle charging stations in fcr markets," *Electric Power Systems Research*, vol. 190, p. 106 667, 2021.
- [5] M. Čičić, C. Vivas, C. Canudas-de-Wit, and F. R. Rubio, "Optimal renewable energy curtailment minimization control using a combined electromobility and grid model," in *IFAC World Congress*, 2023.
- [6] M. Fochesato, C. Cenedese, and J. Lygeros, "A Stackelberg game for incentive-based demand response in energy markets," in *2022 IEEE 61st Conference on Decision and Control (CDC)*, IEEE, 2022, pp. 2487–2492.
- [7] D. Ban, G. Michailidis, and M. Devetsikiotis, "Demand response control for phev charging stations by dynamic price adjustments," in *2012 IEEE PES Innovative Smart Grid Technologies (ISGT)*, IEEE, 2012, pp. 1–8.
- [8] S. Wang, S. Bi, and Y. A. Zhang, "Reinforcement learning for real-time pricing and scheduling control in ev charging stations," *IEEE Transactions on Industrial Informatics*, vol. 17, no. 2, pp. 849–859, 2019.
- [9] M. E. Ben-Akiva, S. R. Lerman, and S. R. Lerman, *Discrete choice analysis: theory and application to travel demand*. MIT press, 1985, vol. 9.
- [10] B. Canizes, J. Soares, A. Costa, *et al.*, "Electric vehicles' user charging behaviour simulator for a smart city," *Energies*, vol. 12, no. 8, p. 1470, 2019.
- [11] Z. Fotouhi, M. R. Hashemi, H. Narimani, and I. S. Bayram, "A general model for ev drivers' charging behavior," *IEEE Transactions on Vehicular Technology*, vol. 68, no. 8, pp. 7368–7382, 2019.
- [12] L. Hu, J. Dong, and Z. Lin, "Modeling charging behavior of battery electric vehicle drivers: A cumulative prospect theory based approach," *Transportation Research Part C: Emerging Technologies*, vol. 102, pp. 474–489, 2019.
- [13] M. Čičić and C. Canudas-de-Wit, "Coupled macroscopic modelling of electric vehicle traffic and energy flows for electromobility control," in *2022 IEEE 61st Conference on Decision and Control (CDC)*, IEEE, 2022, pp. 826–831.